# MIT JOINT PROGRAM
## SCIENCE · POLICY
## GLOBAL CHANGE

# The Equilibrium Climate Response to Sulfur Dioxide and Carbonaceous Aerosol Emissions from East and Southeast Asia

B.S. Grandey, L.K. Yeo, H. Lee and C. Wang

The **MIT Joint Program on the Science and Policy of Global Change** combines cutting-edge scientific research with independent policy analysis to provide a solid foundation for the public and private decisions needed to mitigate and adapt to unavoidable global environmental changes. Being data-driven, the Joint Program uses extensive Earth system and economic data and models to produce quantitative analysis and predictions of the risks of climate change and the challenges of limiting human influence on the environment—essential knowledge for the international dialogue toward a global response to climate change.

To this end, the Joint Program brings together an interdisciplinary group from two established MIT research centers: the **Center for Global Change Science (CGCS)** and the **Center for Energy and Environmental Policy Research (CEEPR)**. These two centers—along with collaborators from the Marine Biology Laboratory (MBL) at

Woods Hole and short- and long-term visitors—provide the united vision needed to solve global challenges.

At the heart of much of the program's work lies MIT's Integrated Global System Model. Through this integrated model, the program seeks to discover new interactions among natural and human climate system components; objectively assess uncertainty in economic and climate projections; critically and quantitatively analyze environmental management and policy proposals; understand complex connections among the many forces that will shape our future; and improve methods to model, monitor and verify greenhouse gas emissions and climatic impacts.

This reprint is intended to communicate research results and improve public understanding of global environment and energy challenges, thereby contributing to informed debate about climate change and the economic and social implications of policy alternatives.

*—Ronald G. Prinn and John M. Reilly,*
*Joint Program Co-Directors*
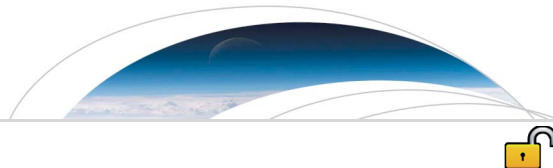
**Key Points:**
- Anthropogenic aerosol emissions from East and Southeast Asia exert a global mean net radiative effect of $-0.49 \pm 0.04$ W/m$^2$
- Strong suppression of precipitation occurs over East and Southeast Asia
- We find no clear evidence of remote effects on precipitation over Australia and West Africa

**Supporting Information:**
- Supporting Information S1

**Correspondence to:**
B. S. Grandey and C. Wang,
benjamin@smart.mit.edu;
wangc@mit.edu

# The Equilibrium Climate Response to Sulfur Dioxide and Carbonaceous Aerosol Emissions From East and Southeast Asia

Benjamin S. Grandey[1] , Lik Khian Yeo[1,2], Hsiang-He Lee[1] , and Chien Wang[1,3]

[1]Center for Environmental Sensing and Modeling, Singapore-MIT Alliance for Research and Technology, Singapore, Singapore, [2]Department of Civil and Environmental Engineering, National University of Singapore, Singapore, Singapore, [3]Center for Global Change Science, Massachusetts Institute of Technology, Cambridge, MA, USA

**Abstract** We investigate the equilibrium climate response to East and Southeast Asian emissions of carbonaceous aerosols and sulfur dioxide, a precursor of sulfate aerosol. Using the Community Earth System Model with the Community Atmosphere Model version 5.3, we find that anthropogenic aerosol emissions from East and Southeast Asia exert a global mean net radiative effect of $-0.49 \pm 0.04$ W/m$^2$. Approximately half of this cooling effect can be attributed to anthropogenic sulfur dioxide emissions. The aerosol emissions drive widespread cooling across the Northern Hemisphere. Strong suppression of precipitation occurs over East and Southeast Asia, indicating that anthropogenic aerosol emissions may impact water resources locally. However, in contrast to previous research, we find no clear evidence of remote effects on precipitation over Australia and West Africa. We recommend further investigation of possible remote effects.

**Plain Language Summary** Aerosols—particles suspended in the atmosphere—influence clouds and the climate system. Using a state-of-the-art global climate model, we investigate the climate impacts of aerosol emissions from human activity in East and Southeast Asia. We find that these aerosol emissions lead to widespread cooling across the Northern Hemisphere and also to reduction of rainfall over East and Southeast Asia, potentially impacting water resources.

## 1. Introduction

Anthropogenic emissions from East and Southeast Asia are responsible for 21% of global sulfur dioxide emissions, 13% of global organic carbon aerosol emissions, and 26% of global black carbon aerosol emissions (Figure 1). These emissions likely influence the climate system by interacting directly with radiation (Haywood & Boucher, 2000) and by interacting with clouds (Fan et al., 2016; Rosenfeld et al., 2014).

In contrast to well-mixed greenhouse gases, the radiative effects of aerosols are regionally heterogeneous. The regional heterogeneity of the aerosol radiative effects likely influences surface temperature gradients and the large-scale distribution of precipitation (Wang, 2015).

Monsoon systems may be particularly sensitive to the heterogeneity of the aerosol radiative effects. For example, several studies have suggested that anthropogenic aerosols influence the East Asian monsoon: the distribution of precipitation over China may be influenced both by absorbing aerosols, such as black carbon (Gu et al., 2006; Jiang et al., 2013; Lau et al., 2006; Menon, 2002), and by sulfate aerosol, via indirect effects on clouds (Guo et al., 2013; Jiang et al., 2013; Liu et al., 2011).

It is likely that the South Asian monsoon is sensitive to absorbing aerosols such as black carbon (Chung et al., 2002; Lau et al., 2006; Lee et al., 2013; Lee & Wang, 2015; Meehl et al., 2008; Ramanathan et al., 2005; Wang et al., 2009), and the South Asian monsoon may be even more sensitive to the indirect effects of sulfate aerosol (Bollasina et al., 2011). Alongside local emission sources, remote emissions sources may contribute to the influence of aerosols on the South Asian monsoon (Bollasina et al., 2014; Cowan & Cai, 2011; Ganguly et al., 2012).

East and Southeast Asian emissions may influence precipitation remotely in other regions by perturbing large-scale circulations (Bartlett et al., 2018). Previous studies have suggested that the Northern Hemisphere aerosol emissions remotely influence the Australian monsoon (Grandey et al., 2016; Rotstayn
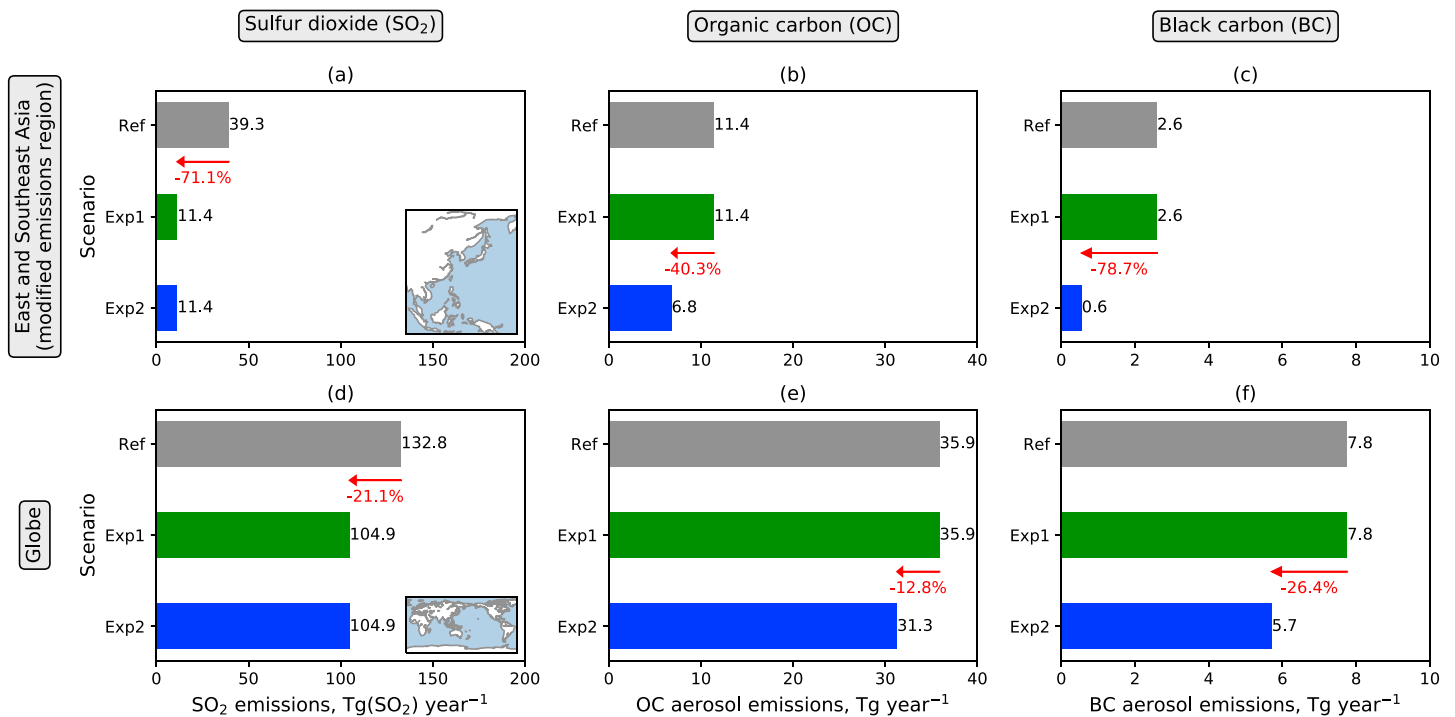
**Figure 1.** Annual emissions of sulfur dioxide (including primary sulfate), organic carbon aerosol, and black carbon aerosol for the three equilibrium scenarios: *Ref* uses year 2000 aerosol emissions; *Exp1* has no anthropogenic sulfur emissions from East and Southeast Asia (94–161°E, 10°S–65°N); *Exp2* has no anthropogenic aerosol emissions from East and Southeast Asia. Red arrows and text indicate modifications to the emissions in the experimental scenarios. (a)–(c) Emissions from East and Southeast Asia; (d)–(f) global emissions. The emissions include both anthropogenic and natural sources. Of the sulfur dioxide, 2.5% is emitted as primary sulfate.

et al., 2012) and the West African monsoon (Bartlett et al., 2018; Booth et al., 2012; Dong et al., 2014; Grandey et al., 2016).

In this letter, we explore the equilibrium climate response to anthropogenic aerosol emissions from East and Southeast Asia. We consider the influence of both sulfate aerosol and carbonaceous aerosols. To our knowledge, this is the first study to assess the cloud radiative effects and equilibrium climate impacts of anthropogenic sulfur dioxide and carbonaceous aerosol emissions from East and Southeast Asia.

Based on the exploratory research of Grandey et al. (2016; henceforth *G16*)—who investigated the transient climate response to aerosol emissions from a larger Asia region—we hypothesize that the anthropogenic aerosol emissions from East and Southeast Asia will (1) drive widespread cooling of the Northern Hemisphere, leading to interhemispheric asymmetry in the surface temperature response; (2) suppress precipitation in the Northern Hemisphere tropics and weakly enhance precipitation in the Southern Hemisphere tropics; (3) suppress East Asian monsoon precipitation; (4) suppress South Asian monsoon precipitation, especially over southern India; (5) enhance Australian monsoon precipitation; and (6) suppress West African monsoon precipitation over the Sahel. These hypotheses are discussed and tested in section 4.

## 2. Methods

### 2.1. Scenarios

The three scenarios differ only in their aerosol emissions (Figure 1):

1. *Ref*, the reference scenario, uses year 2000 emissions (supplement of Lamarque et al., 2010; Liu et al., 2012).
2. *Exp1*, the first experimental scenario, has no anthropogenic emissions of sulfur dioxide (including primary sulfate) from East and Southeast Asia: sulfur dioxide emissions from all anthropogenic sectors, including shipping, are removed within the regional bounds of 94–161°E, 10°S–65°N. Comparison of *Exp1* with *Ref* reveals the influence of anthropogenic sulfur dioxide emissions from East and Southeast Asia, assuming all other emissions remain at year 2000 levels.

3. *Exp2*, the second experimental scenario, has no anthropogenic emissions of aerosol (sulfur dioxide, organic carbon, and black carbon) from East and Southeast Asia. Comparison of *Exp2* with *Ref* reveals the influence of anthropogenic aerosol emissions from East and Southeast Asia.

## 2.2. Model Configuration

Simulations are performed using the Community Earth System Model version 1.2.2, with the Community Atmosphere Model version 5.3 (CAM5.3) and an aerosol module with three log-normal modes (MAM3; Liu et al., 2012). Depending on the mode—Aitken, accumulation, or coarse—MAM3 simulates an internal mixture of sulfate, primary organic matter, secondary organic matter, black carbon, sea salt, and soil dust. For each mode, both mass concentration and number concentration are tracked. In addition to interacting with radiation, the modeled aerosols interact with stratiform clouds via nucleation schemes for both liquid and ice cloud particles, influencing precipitation formation via autoconversion (Gettelman et al., 2010; Morrison & Gettelman, 2008). Liu et al. (2012) describe MAM3 and compare the simulated aerosol fields with observations; Ghan et al. (2012) assess the anthropogenic aerosol radiative effects. The indirect effects via stratiform clouds are particularly strong (Ghan et al., 2012), leading to a relatively strong aerosol effective radiative forcing compared with other global climate models (Shindell et al., 2013).

CAM5.3 is run at a horizontal resolution of $1.9° \times 2.5°$ with 30 levels in the vertical direction. Greenhouse gas concentrations are prescribed using year 2000 climatological values.

For each emissions scenario, two simulations are performed: a simulation using prescribed sea surface temperatures (SSTs) and a simulation using a coupled atmosphere-ocean configuration.

The prescribed SST simulations facilitate diagnosis of aerosol radiative effects (Ghan, 2013). The configuration follows the *F_2000_CAM5* component set. Each prescribed SST simulation is run for 32 years: the first 2 years are excluded from the analysis; the final 30 years are analyzed.

The coupled atmosphere-ocean simulations facilitate investigation of the equilibrium climate response to changes in the aerosol emissions. The configuration follows the *B_2000_CAM5_CN* component set. The three-dimensional ocean model uses a displaced pole grid with a resolution of approximately $1° \times 1°$. Each coupled atmosphere-ocean simulation is run for 100 years: the first 40 years, during which the simulation moves toward a near-equilibrium state, are excluded from the analysis; the final 60 years are analyzed.

## 2.3. Data From Grandey et al. (2016; G16)

Data from the transient simulations (*RCP4.5* and *A2x*; 2080–2099) and prescribed SST simulations (*pRCP4.5* and *pA2x*) of G16 are also analyzed. These simulations are described by G16. Table S1 in the supporting information summarizes the differences between the G16 transient scenarios (*RCP4.5* and *A2x*) and the equilibrium scenarios of the present manuscript (*Ref*, *Exp1*, and *Exp2*).

In the present study, the analysis methodology differs slightly from that of G16: the analysis uses calendar years (rather than years starting in December), and when calculating radiative effects using the prescribed SST simulations (*pRCP4.5* and *pA2x*), the first 2 years are discarded providing an analysis period of 13 years (rather than 12 years). Therefore, the G16 simulation results presented in this manuscript may differ slightly from those presented by G16.

## 2.4. Global Precipitation Climatology Project Data

The Global Precipitation Climatology Project (GPCP) version 2.3 combined precipitation data set provides an observational estimate of monthly precipitation at $2.5° \times 2.5°$ resolution globally, based on analysis of satellite-retrieved data and rain gauge observations (Adler et al., 2003). Monthly long-term mean GPCP data, averaged across 1981–2010, are used to validate the seasonal and latitudinal distribution of precipitation produced by the *Ref* simulation over the four regions discussed in section 4.

Compared to GPCP, *Ref* reproduces the East Asian monsoon, although peak precipitation in June occurs slightly too far south over East Asia (Figures S5a and S5b). *Ref* also reproduces the South Asian monsoon, although monsoon precipitation is overestimated over both northern and southern South Asia (Figures S7a and S7b). *Ref* accurately reproduces the Australian monsoon, although monsoon precipitation is overestimated over northern Australia (Figures S9a and S9b). *Ref* accurately reproduces the West African monsoon precipitation, resulting in close agreement between *Ref* and GPCP over the Sahel (Figures S11a and S11b).
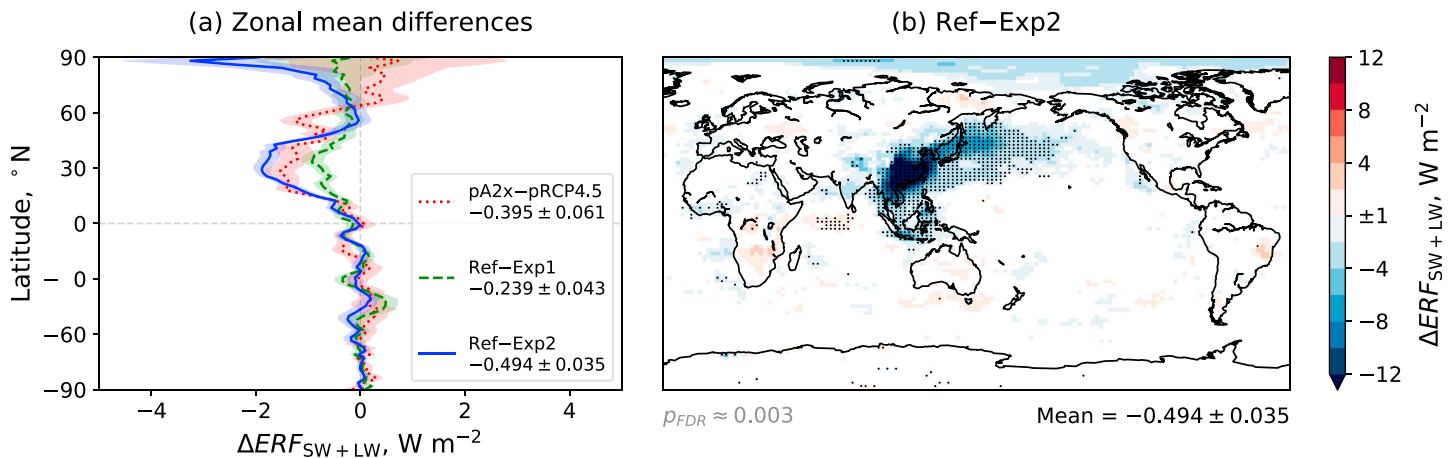
**Figure 2.** Differences in annual mean aerosol effective radiative forcing ($ERF_{SW+LW}$), diagnosed using the prescribed sea surface temperature simulations. (a) Zonal mean differences in $ERF_{SW+LW}$ for different pairs of scenarios. Shading indicates combined standard errors, calculated using the annual zonal means for each simulation year. The legend contains global area-weighted mean differences and associated combined standard errors, calculated using the annual global means for each simulation year. (b) Map of *Ref-Exp2* differences in $ERF_{SW+LW}$. White indicates differences with a magnitude less than the threshold value at the center of the color bar ($\pm 1$ W/m$^2$). For locations where the magnitude is greater than this threshold value, stippling indicates differences that are statistically significant at a significance level of 0.05 after controlling the false discovery rate (Benjamini & Hochberg, 1995; Wilks, 2016); the two-tailed *p* values are generated by a two-sample *t* test, assuming equal population variances, using annual mean data from each simulation year as the input; the approximate *p* value threshold ($p_{FDR}$), which takes the false discovery rate into account, is written beneath the map. The global area-weighted mean difference is also written beneath the map.

## 3. Results

### 3.1. Radiative Effects

The anthropogenic sulfur dioxide emissions from East and Southeast Asia exert a net cooling effect on the climate system, contributing $-0.24 \pm 0.04$ W/m$^2$ to the net effective radiative forcing (Figure 2a). The net radiative effect is dominated by the shortwave cloud radiative effect ($-0.44 \pm 0.04$ W/m$^2$; Figure S1a) and the longwave cloud radiative effect ($+0.26 \pm 0.02$ W/m$^2$; Figure S2a). The direct radiative effect ($-0.03 \pm 0.01$ W/m$^2$; Figure S3a) and the surface albedo radiative effect ($-0.04 \pm 0.02$ W/m$^2$; Figure S4a) are much smaller.

When carbonaceous aerosol emissions are also modified, the anthropogenic aerosol emissions exert an even stronger net radiative effect of $-0.49 \pm 0.04$ W/m$^2$, twice as strong as when only the sulfur dioxide emissions are modified. The shortwave cloud radiative effect becomes stronger ($-0.66 \pm 0.03$ W/m$^2$): in MAM3, organic carbon aerosol is internally mixed with other species of high hygroscopicity and therefore contributes efficiently to cloud condensation nuclei availability (Grandey et al., 2018). Counterintuitively, the longwave cloud radiative effect becomes weaker ($+0.18 \pm 0.02$ W/m$^2$): this is unexpected, because neither organic carbon aerosol nor black carbon aerosol acts as ice nuclei in CAM5.3 (Gettelman et al., 2010). The direct radiative effect becomes positive ($+0.03 \pm 0.01$ W/m$^2$), due to absorption by black carbon aerosol.

The longwave cloud radiative effect (Figure S2b) of the anthropogenic aerosol emissions is strongest over Southeast Asia, the South China Sea, the Bay of Bengal, and the eastern Indian Ocean—in the tropics. In contrast, the shortwave cloud radiative effect (Figure S1b) and the net radiative effect (Figure 2b) are strongest over East Asia and the western North Pacific Ocean—in the Northern Hemisphere subtropics and midlatitudes. The net radiative effect exhibits strong interhemispheric asymmetry.

### 3.2. Surface Temperature

The interhemispheric asymmetry in the net radiative effect drives interhemispheric asymmetry in the surface temperature response (Figure 3). The East and Southeast Asian aerosol emissions drive widespread cooling of the Northern Hemisphere, especially in the midlatitudes and the Arctic. The aerosol emissions also cool parts of the Southern Hemisphere, but the cooling is generally not as strong as in the Northern Hemisphere.

When both carbonaceous and sulfur emissions are modified, the global mean cooling ($-0.19 \pm 0.03$ °C) is approximately twice as strong as when only sulfur emissions are modified ($-0.10 \pm 0.03$ °C). As mentioned above, the net radiative effects for the two experimental cases also differ by a factor of 2. Hence, the

## (a) Zonal mean differences

## (b) Ref−Exp2
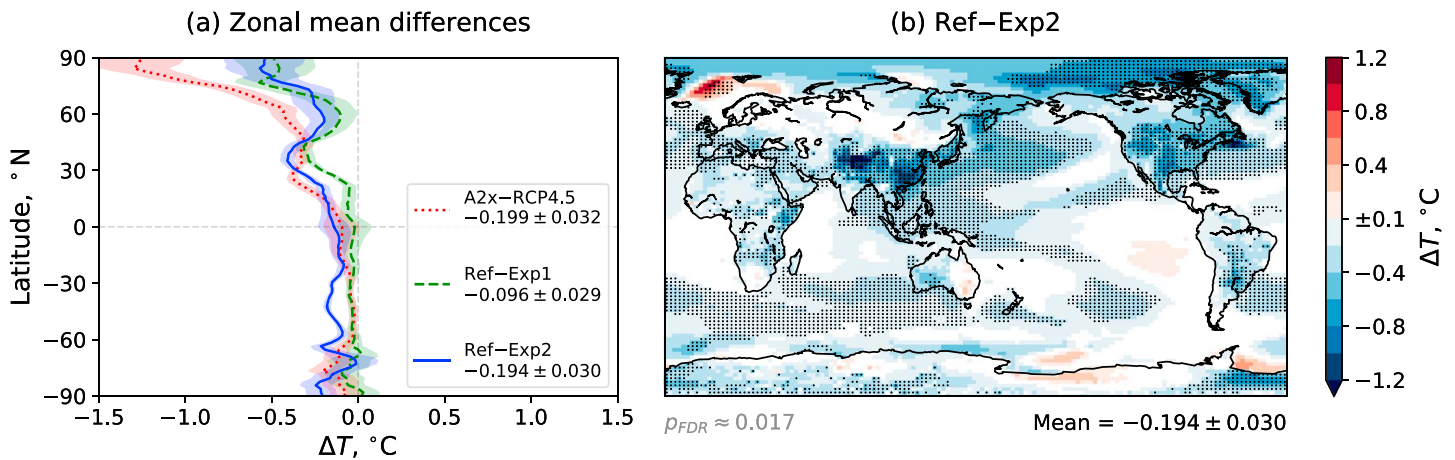


**Figure 3.** Differences in annual mean surface temperature (*T*) for the coupled atmosphere-ocean simulations. The figure components are explained in the caption of Figure 2.

relationship between the net radiative effect and the global mean temperature response is linear: both experimental cases produce a sensitivity of 0.4 °C/(W/m$^2$).
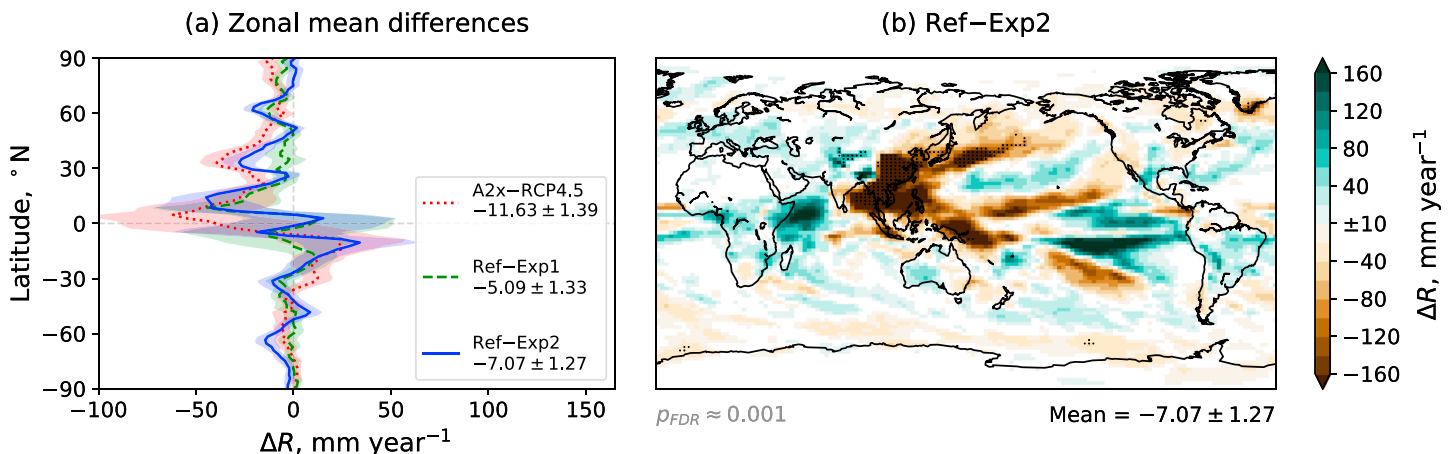
### 3.3. Precipitation

Precipitation is sensitive to changes in surface temperature gradients (Chiang & Friedman, 2012; Wang, 2015). The interhemispheric asymmetry in the surface temperature response drives interhemispheric asymmetry in the precipitation response: in particular, the East and Southeast Asian aerosol emissions suppress precipitation in the Northern Hemisphere (Figure 4a). Precipitation is strongly suppressed over East and Southeast Asia; precipitation is enhanced over the western Indian Ocean and over parts of the eastern Pacific Ocean, but statistical significance is generally absent (Figure 4b). We further discuss the regional precipitation response in section 4 below.

## 4. Discussion and Recommendations

In section 1 we stated six hypotheses regarding the influence of anthropogenic aerosol emissions from East and Southeast Asia, based on the conclusions of G16. We now discuss and test these hypotheses.

First, we hypothesized that the emissions would drive widespread cooling of the Northern Hemisphere, leading to interhemispheric asymmetry in the surface temperature response. Our results support this hypothesis: the interhemispheric asymmetry in the net radiative effect (Figure 2) drives interhemispheric asymmetry in the surface temperature response (Figure 3).

## (a) Zonal mean differences

## (b) Ref−Exp2



**Figure 4.** Differences in annual total precipitation rate (*R*) for the coupled atmosphere-ocean simulations. The figure components are explained in the caption of Figure 2.

Second, we hypothesized that the emissions would (i) suppress precipitation in the Northern Hemisphere tropics and (ii) weakly enhance precipitation in the Southern Hemisphere tropics. Such a precipitation response would be consistent with a southward shift of the intertropical convergence zone in response to the cooling of the Northern Hemisphere (Chiang & Friedman, 2012). Our results support the first part of this hypothesis: precipitation is suppressed in the Northern Hemisphere tropics (Figure 4a). However, due to the large standard errors, our results do not provide conclusive evidence that precipitation is enhanced in the Southern Hemisphere tropics.

Third, we hypothesized that the aerosol emissions would suppress East Asian monsoon precipitation. Our results support this hypothesis: annual precipitation is suppressed over East Asia (Figure 4b); the suppression occurs throughout the year, especially during the summer monsoon months (Figure S5c). Surface cooling likely contributes to the suppression of precipitation (Jiang et al., 2013). In agreement with G16, the suppression of precipitation is also associated with anomalous downward motion (often indicating suppressed ascent) in the midtroposphere between 25° and 35°N, although statistical significance is absent (Figure S6b); anomalous upward motion (generally indicating suppressed descent) occurs between 35° and 45°N.

Fourth, we hypothesized that the aerosol emissions would suppress South Asian monsoon precipitation, especially over southern India. Our results provide only weak support for this hypothesis: annual precipitation is suppressed over southern India, but significance is absent (Figure 4b). The suppression of precipitation over southern South Asia only occurs during January–July, with suppression over central South Asia during August, and enhancement over much of South Asia during September–December (Figure S7c). (The precipitation response is correlated with the midtropospheric motion anomalies, shown in Figure S8b.) G16—who modified the aerosol emissions over South Asia alongside other parts of Asia—reported much stronger suppression of precipitation over southern South Asia: this apparent discrepancy between the two studies suggests that local South Asian emissions contribute to the suppression reported by G16. However, when we reanalyze the G16 transient simulation data, taking the false discovery rate into account (Wilks, 2016), we find that the suppression reported by G16 lacks statistical significance (Figure S7d): therefore, the apparent discrepancy can largely be explained by differing statistical methodology.

Fifth, we hypothesized that the aerosol emissions would enhance Australian monsoon precipitation. Our results do not support this hypothesis: although weak enhancement of annual precipitation occurs over western Australia (Figure 4b), there is no clear enhancement of the austral monsoon precipitation or circulation over northern Australia (Figures S9c, S10b). When we reanalyze the G16 transient simulation data, we find that the enhancement reported by G16 lacks statistical significance (Figure S9d).

Sixth, we hypothesized that the aerosol emissions would suppress West African monsoon precipitation over the Sahel. Again, our results do not support this hypothesis: annual precipitation is not suppressed over the Sahel (Figure 4b); there is no suppression during the summer monsoon months, except during September (Figure S11c). However, there are two similarities with the results of G16 in the vicinity of West Africa: the aerosols appear to drive a slight southward shift of the intertropical convergence zone (Figures S11c, d) and also a slight weakening of the West African westerly jet (Pu & Cook, 2012) during September and October (Figure S12b), although significance is absent. Significance is also absent for the G16 transient simulation precipitation data if the false discovery rate is controlled (Figure S11d).

To summarize, we find interhemispheric asymmetry in the radiative effects, surface temperature response, and precipitation response, in agreement with the results of G16. We also find local suppression of precipitation over East Asia, again in agreement with G16. However, diverging from G16, we do not find clear evidence of remote effects, especially over Australia and the Sahel. These discrepancies can largely be explained by the increased statistical rigor we newly apply in the current study: if the false discovery rate is controlled, resulting in a more rigorous $p$ value threshold, statistical significance is absent for many of the precipitation features reported by G16 (Figures S7d, S9d, and S11d). Our analysis supports the argument of Wilks (2016), who highlighted the importance of controlling the false discovery rate.

Considering the methodological differences between the two studies (Table S1), other factors may also contribute to the differences between the transient simulation results of G16 and the equilibrium simulation results described in this paper. First, the long-term equilibrium climate impacts likely differ from shorter-term transient climate impacts. Second, South Asian emissions may play an important role in the suppression of

the South Asian monsoon and some remote effects outside Asia. Third, nonlinear interactions between aerosol emissions from Asia, aerosol emissions outside Asia, and greenhouse gas forcing may also influence the local and remote impacts of the aerosol emissions.

We recommend further investigation of proposed remote effects. Exploratory research—such as that presented by G16—helps us to formulate hypotheses, but the risk of spurious results should be acknowledged. Exploratory research should be followed by research that tests clearly formulated hypotheses, as we have attempted to do in this letter. Hypotheses should ultimately be tested using a range of different climate models, in order to assess the impact of uncertainty associated with aerosol-cloud interactions. Methods that increase statistical rigor—such as the method advocated by Wilks (2016)—should also be implemented. Confirmation of hypotheses is valuable; negation of hypotheses is even more valuable, revealing the need for further research.

## 5. Summary and Conclusions

Our results suggest that anthropogenic aerosol emissions from East and Southeast Asia exert a net radiative effect of $-0.49 \pm 0.04$ W/m$^2$ on the climate system, largely due to indirect effects via clouds. Sulfur dioxide emissions are responsible for approximately half of the net radiative effect.

Although the radiative effects are concentrated in the vicinity of the source region, the sea-surface temperature response facilitates widespread cooling of the Northern Hemisphere. The cooling of the Northern Hemisphere drives suppression of rainfall in the Northern Hemisphere tropics.

Strong suppression of rainfall occurs over the source region of East and Southeast Asia. However, we find no clear evidence of remote effects on the Australian monsoon and the West African monsoon, although such remote effects cannot be ruled out. As discussed in the final paragraph of section 4, we recommend further investigation of possible remote effects.

We conclude that anthropogenic aerosol emissions may influence rainfall across East and Southeast Asia. The potential impact on water resources in Southeast Asia is the focus of an ongoing study.

### Code and Data Availability

Community Earth System Model 1.2.2 is available via http://www.cesm.ucar.edu/models/cesm1.2/. Model namelist files, configuration scripts, and analysis code are available via https://github.com/grandey/p17d-sulphur-eas-eqm, archived at https://doi.org/10.5281/zenodo.1400401. The *Ref*, *Exp1*, and *Exp2* simulation data analyzed in this paper are archived at https://doi.org/10.6084/m9.figshare.6072887. The G16 simulation data are archived at https://doi.org/10.6084/m9.figshare.2067084. The GPCP precipitation data were provided by the NOAA/OAR/ESRL PSD, Boulder, CO, USA, from their website at https://www.esrl.noaa.gov/psd/.

### Author Contributions

B. S. G. and L. K. Y. designed the experiment, with contributions from H. H. L. and C. W. B. S. G. configured the simulations and analyzed the results. B. S. G. wrote the manuscript, with contributions from L. K. Y., H. H. L., and C. W.

### References

Adler, R. F., Huffman, G. J., Chang, A., Ferraro, R., Xie, P.-P., Janowiak, J., et al. (2003). The version-2 Global Precipitation Climatology Project (GPCP) monthly precipitation analysis (1979–present). *Journal of Hydrometeorology*, 4(6), 1147–1167. https://doi.org/10.1175/1525-7541(2003)004<1147:TVGPCP>2.0.CO;2

Bartlett, R. E., Bollasina, M. A., Booth, B. B. B., Dunstone, N. J., Marenco, F., Messori, G., & Bernie, D. J. (2018). Do differences in future sulfate emission pathways matter for near-term climate? A case study for the Asian monsoon. *Climate Dynamics*, 50(5–6), 1863–1880. https://doi.org/10.1007/s00382-017-3726-6

Benjamini, Y., & Hochberg, Y. (1995). Controlling the false discovery rate: A practical and powerful approach to multiple testing. *Journal of the Royal Statistical Society, Series B*, 57(1), 289–300.

Bollasina, M. A., Ming, Y., & Ramaswamy, V. (2011). Anthropogenic aerosols and the weakening of the South Asian summer monsoon. *Science*, 334(6055), 502–505. https://doi.org/10.1126/science.1204994

Bollasina, M. A., Ming, Y., Ramaswamy, V., Schwarzkopf, M. D., & Naik, V. (2014). Contribution of local and remote anthropogenic aerosols to the twentieth century weakening of the South Asian Monsoon. *Geophysical Research Letters*, 41, 680–687. https://doi.org/10.1002/2013GL058183

Booth, B. B. B., Dunstone, N. J., Halloran, P. R., Andrews, T., & Bellouin, N. (2012). Aerosols implicated as a prime driver of twentieth-century North Atlantic climate variability. *Nature*, 484(7393), 228–232. https://doi.org/10.1038/nature10946

Chiang, J. C. H., & Friedman, A. R. (2012). Extratropical cooling, interhemispheric thermal gradients, and tropical climate change. *Annual Review of Earth and Planetary Sciences*, *40*(1), 383–412. https://doi.org/10.1146/annurev-earth-042711-105545

Chung, C. E., Ramanathan, V., & Kiehl, J. T. (2002). Effects of the South Asian absorbing haze on the northeast monsoon and surface–air heat exchange. *Journal of Climate*, *15*(17), 2462–2476. https://doi.org/10.1175/1520-0442(2002)015<2462:EOTSAA>2.0.CO;2

Cowan, T., & Cai, W. (2011). The impact of Asian and non-Asian anthropogenic aerosols on 20th century Asian summer monsoon. *Geophysical Research Letters*, *38*, L11703. https://doi.org/10.1029/2011GL047268

Dong, B., Sutton, R. T., Highwood, E., & Wilcox, L. (2014). The impacts of European and Asian anthropogenic sulfur dioxide emissions on Sahel rainfall. *Journal of Climate*, *27*, 7000–7017. https://doi.org/10.1175/JCLI-D-13-00769.1

Fan, J., Wang, Y., Rosenfeld, D., & Liu, X. (2016). Review of aerosol–cloud interactions: Mechanisms, significance, and challenges. *Journal of the Atmospheric Sciences*, *73*(11), 4221–4252. https://doi.org/10.1175/JAS-D-16-0037.1

Ganguly, D., Rasch, P. J., Wang, H., & Yoon, J.-H. (2012). Climate response of the South Asian monsoon system to anthropogenic aerosols. *Journal of Geophysical Research*, *117*, D13209. https://doi.org/10.1029/2012JD017508

Gettelman, A., Liu, X., Ghan, S. J., Morrison, H., Park, S., Conley, A. J., et al. (2010). Global simulations of ice nucleation and ice supersaturation with an improved cloud scheme in the Community Atmosphere Model. *Journal of Geophysical Research*, *115*, D18216. https://doi.org/10.1029/2009JD013797

Ghan, S. J. (2013). Technical Note: Estimating aerosol effects on cloud radiative forcing. *Atmospheric Chemistry and Physics*, *13*(19), 9971–9974. https://doi.org/10.5194/acp-13-9971-2013

Ghan, S. J., Liu, X., Easter, R. C., Zaveri, R., Rasch, P. J., Yoon, J.-H., & Eaton, B. (2012). Toward a minimal representation of aerosols in climate models: Comparative decomposition of aerosol direct, semidirect, and indirect radiative forcing. *Journal of Climate*, *25*(19), 6461–6476. https://doi.org/10.1175/JCLI-D-11-00650.1

Grandey, B. S., Cheng, H., & Wang, C. (2016). Transient climate impacts for scenarios of aerosol emissions from Asia: A story of coal versus gas. *Journal of Climate*, *29*(8), 2849–2867. https://doi.org/10.1175/JCLI-D-15-0555.1

Grandey, B. S., Rothenberg, D., Avramov, A., Jin, Q., Lee, H.-H., Liu, X., et al. (2018). Effective radiative forcing in the aerosol–climate model CAM5.3-MARC-ARG. *Atmospheric Chemistry and Physics Discussions*, 1–39. https://doi.org/10.5194/acp-2018-118

Gu, Y., Liou, K. N., Xue, Y., Mechoso, C. R., Li, W., & Luo, Y. (2006). Climatic effects of different aerosol types in China simulated by the UCLA general circulation model. *Journal of Geophysical Research*, *111*(D15), D15201. https://doi.org/10.1029/2005JD006312

Guo, L., Highwood, E. J., Shaffrey, L. C., & Turner, A. G. (2013). The effect of regional changes in anthropogenic aerosols on rainfall of the East Asian Summer Monsoon. *Atmospheric Chemistry and Physics*, *13*(3), 1521–1534. https://doi.org/10.5194/acp-13-1521-2013

Haywood, J., & Boucher, O. (2000). Estimates of the direct and indirect radiative forcing due to tropospheric aerosols: A review. *Reviews of Geophysics*, *38*(4), 513–543. https://doi.org/10.1029/1999RG000078

Jiang, Y., Liu, X., Yang, X.-Q., & Wang, M. (2013). A numerical study of the effect of different aerosol types on East Asian summer clouds and precipitation. *Atmospheric Environment*, *70*, 51–63. https://doi.org/10.1016/j.atmosenv.2012.12.039

Lamarque, J.-F., Bond, T. C., Eyring, V., Granier, C., Heil, A., Klimont, Z., et al. (2010). Historical (1850–2000) gridded anthropogenic and biomass burning emissions of reactive gases and aerosols: Methodology and application. *Atmospheric Chemistry and Physics*, *10*(15), 7017–7039. https://doi.org/10.5194/acp-10-7017-2010

Lau, K. M., Kim, M. K., & Kim, K. M. (2006). Asian summer monsoon anomalies induced by aerosol direct forcing: The role of the Tibetan Plateau. *Climate Dynamics*, *26*(7–8), 855–864. https://doi.org/10.1007/s00382-006-0114-z

Lee, S.-Y., Shin, H.-J., & Wang, C. (2013). Nonlinear effects of coexisting surface and atmospheric forcing of anthropogenic absorbing aerosols: Impact on the south asian monsoon onset. *Journal of Climate*, *26*(15), 5594–5607. https://doi.org/10.1175/JCLI-D-12-00741.1

Lee, S.-Y., & Wang, C. (2015). The response of the South Asian summer monsoon to temporal and spatial variations in absorbing aerosol radiative forcing. *Journal of Climate*, *28*(17), 6626–6646. https://doi.org/10.1175/JCLI-D-14-00609.1

Liu, X., Easter, R. C., Ghan, S. J., Zaveri, R., Rasch, P., Shi, X., et al. (2012). Toward a minimal representation of aerosols in climate models: Description and evaluation in the Community Atmosphere Model CAM5. *Geoscientific Model Development*, *5*(3), 709–739. https://doi.org/10.5194/gmd-5-709-2012

Liu, X., Xie, X., Yin, Z.-Y., Liu, C., & Gettelman, A. (2011). A modeling study of the effects of aerosols on clouds and precipitation over East Asia. *Theoretical and Applied Climatology*, *106*(3–4), 343–354. https://doi.org/10.1007/s00704-011-0436-6

Meehl, G. A., Arblaster, J. M., & Collins, W. D. (2008). Effects of black carbon aerosols on the Indian monsoon. *Journal of Climate*, *21*(12), 2869–2882. https://doi.org/10.1175/2007JCLI1777.1

Menon, S. (2002). Climate effects of black carbon aerosols in China and India. *Science*, *297*(5590), 2250–2253. https://doi.org/10.1126/science.1075159

Morrison, H., & Gettelman, A. (2008). A new two-moment bulk stratiform cloud microphysics scheme in the Community Atmosphere Model, version 3 (CAM3). Part I: Description and numerical tests. *Journal of Climate*, *21*(15), 3642–3659. https://doi.org/10.1175/2008JCLI2105.1

Pu, B., & Cook, K. H. (2012). Role of the West African westerly jet in Sahel rainfall variations. *Journal of Climate*, *25*(8), 2880–2896. https://doi.org/10.1175/JCLI-D-11-00394.1

Ramanathan, V., Chung, C., Kim, D., Bettge, T., Buja, L., Kiehl, J. T., et al. (2005). Atmospheric brown clouds: Impacts on South Asian climate and hydrological cycle. *Proceedings of the National Academy of Sciences*, *102*(15), 5326–5333. https://doi.org/10.1073/pnas.0500656102

Rosenfeld, D., Andreae, M. O., Asmi, A., Chin, M., de Leeuw, G., Donovan, D. P., et al. (2014). Global observations of aerosol-cloud-precipitation-climate interactions. *Reviews of Geophysics*, *52*, 750–808. https://doi.org/10.1002/2013RG000441

Rotstayn, L. D., Jeffrey, S. J., Collier, M. A., Dravitzki, S. M., Hirst, A. C., Syktus, J. I., & Wong, K. K. (2012). Aerosol- and greenhouse gas-induced changes in summer rainfall and circulation in the Australasian region: A study using single-forcing climate simulations. *Atmospheric Chemistry and Physics*, *12*(14), 6377–6404. https://doi.org/10.5194/acp-12-6377-2012

Shindell, D. T., Lamarque, J.-F., Schulz, M., Flanner, M., Jiao, C., Chin, M., et al. (2013). Radiative forcing in the ACCMIP historical and future climate simulations. *Atmospheric Chemistry and Physics*, *13*(6), 2939–2974. https://doi.org/10.5194/acp-13-2939-2013

Wang, C. (2015). Anthropogenic aerosols and the distribution of past large-scale precipitation change. *Geophysical Research Letters*, *42*, 10,876–10,884. https://doi.org/10.1002/2015GL066416

Wang, C., Kim, D., Ekman, A. M. L., Barth, M. C., & Rasch, P. J. (2009). Impact of anthropogenic aerosols on Indian summer monsoon. *Geophysical Research Letters*, *36*, L21704. https://doi.org/10.1029/2009GL040114

Wilks, D. S. (2016). "The stippling shows statistically significant grid points": How research results are routinely overstated and overinterpreted, and what to do about it. *Bulletin of the American Meteorological Society*, *97*(12), 2263–2273. https://doi.org/10.1175/BAMS-D-15-00267.1

# Joint Program Reprint Series - Recent Articles

**2018-14    The Equilibrium Climate Response to Sulfur Dioxide and Carbonaceous Aerosol Emissions from East and Southeast Asia.** Grandey, B.S., L.K. Yeo, H. Lee and C. Wang, *Geophysical Research Letters* 45 (doi:10.1029/2018GL080127) (2018)

**2018-13    The Impact of Climate Change Policy on the Risk of Water Stress in Southern and Eastern Asia.** Gao, X., C.A. Schlosser, C. Fant and K. Strzepek *Environmental Research Letters* 13(6): 4039 (2018)

**2018-12    On the representation of aerosol activation and its influence on model-derived estimates of the aerosol indirect effect.** Rothenberg, D., A. Avramov and C. Wang, *Atmospheric Chemistry & Physics* 18: 7961–7983 (2018)

**2018-11    The greening of Northwest Indian subcontinent and reduction of dust abundance resulting from Indian summer monsoon revival.** Jin, Q., and C. Wang, *Scientific Reports* 8: 4573 (2018)

**2018-10    Description and Evaluation of the MIT Earth System Model (MESM).** Sokolov, A., D. Kicklighter, A. Schlosser, C. Wang, E. Monier, B. Brown-Steiner, R. Prinn, C. Forest, X. Gao, A. Libardoni and S. Eastham, *Journal of Advances in Modeling Earth Systems* 10(8): 1759–1789 (2018)

**2018-9    Maximizing Ozone Signals Among Chemical, Meteorological, and Climatological Variability.** Brown-Steiner, B., N.E. Selin, R.G. Prinn, E. Monier, S. Tilmes, L. Emmons and F. Garcia-Menendez, *Atmospheric Chemistry & Physics* 18: 8373–8388 (2018)

**2018-8    New data for representing irrigated agriculture in economy-wide models.** Ledvina, K., N. Winchester, K. Strzepek and J.M. Reilly, *Journal of Global Economic Analysis* 3(1): 122–155 (2018)

**2018-7    Sectoral aggregation error in the accounting of energy and emissions embodied in trade and consumption.** Zhang, D., J. Caron and N. Winchester, *Journal of Industrial Ecology*, online first (doi: 10.1111/jiec.12734) (2018)

**2018-6    Potential Impacts of Climate Warming and Changing Hot Days on the Electric Grid: A Case Study for a Large Power Transformer (LPT) in the Northeast United States.** Gao, X., C.A. Schlosser and E. Morgan, *Climatic Change* 147(1-2): 107–118 (2018)

**2018-5    Toward a consistent modeling framework to assess multi-sectoral climate impacts.** Monier, E., S. Paltsev, A. Sokolov, Y.-H.H. Chen, X. Gao, Q. Ejaz, E. Couzo, C. Schlosser, S. Dutkiewicz, C. Fant, J. Scott, D. Kicklighter, J. Morris, H. Jacoby, R. Prinn and M. Haigh, *Nature Communications* 9: 660 (2018)

**2018-4    Tight Oil Market Dynamics: Benchmarks, Breakeven Points, and Inelasticities.** Kleinberg, R.L., S. Paltsev, C.K.E. Ebinger, D.A. Hobbs and T. Boersma, *Energy Economics* 70: 70–83 (2018)

**2018-3    The Impact of Water Scarcity on Food, Bioenergy and Deforestation.** Winchester, N., K. Ledvina, K. Strzepek and J.M. Reilly, *Australian Journal of Agricultural and Resource Economics*, online first (doi:10.1111/1467-8489.12257) (2018)

**2018-2    Modelling Ocean Colour Derived Chlorophyll-a.** Dutkiewicz, S., A.E. Hickman and O. Jahn, *Biogeosciences* 15: 613–630 (2018)

**2018-1    Hedging Strategies: Electricity Investment Decisions under Policy Uncertainty.** Morris, J., V. Srikrishnan, M. Webster and J. Reilly, *Energy Journal*, 39(1) (2018)

**2017-24    Towards a Political Economy Framework for Wind Power: Does China Break the Mould?.** Karplus, V.J., M. Davidson and F. Kahrl, Chapter 13 in: *The Political Economy of Clean Energy Transitions*, D. Arent, C. Arent, M. Miller, F. Tarp, O. Zinaman (eds.), UNU-WIDER/Oxford University Press, Helsinki, Finland (2017)

**2017-23    Carbon Pricing under Political Constraints: Insights for Accelerating Clean Energy Transitions.** Karplus, V.J. and J. Jenkins, Chapter 3 in: *The Political Economy of Clean Energy Transitions*, D. Arent, C. Arent, M. Miller, F. Tarp, O. Zinaman (eds.), UNU-WIDER/Oxford University Press, Helsinki, Finland (2017)

**2017-22    "Climate response functions" for the Arctic Ocean: a proposed coordinated modelling experiment.** Marshall, J., J. Scott and A. Proshutinsky, *Geoscientific Model Development* 10: 2833–2848 (2017)

**2017-21    Aggregation of gridded emulated rainfed crop yield projections at the national or regional level.** Blanc, É., *Journal of Global Economic Analysis* 2(2): 112–127 (2017)

**2017-20    Historical greenhouse gas concentrations for climate modelling (CMIP6).** Meinshausen, M., E. Vogel, A. Nauels, K. Lorbacher, N. Meinshausen, D. Etheridge, P. Fraser, S.A. Montzka, P. Rayner, C. Trudinger, P. Krummel, U. Beyerle, J.G. Cannadell, J.S. Daniel, I. Enting, R.M. Law, S. O'Doherty, R.G. Prinn, S. Reimann, M. Rubino, G.J.M. Velders, M.K. Vollmer, and R. Weiss, *Geoscientific Model Development* 10: 2057–2116 (2017)

**2017-19    The Future of Coal in China.** Zhang, X., N. Winchester and X. Zhang, *Energy Policy,* 110: 644–652 (2017)

**2017-18    Developing a Consistent Database for Regional Geologic CO2 Storage Capacity Worldwide.** Kearns, J., G. Teletzke, J. Palmer, H. Thomann, H. Kheshgi, H. Chen, S. Paltsev and H. Herzog, *Energy Procedia*, 114: 4697–4709 (2017)

---